Amirkabir University of Technology
(Tehran Polytechnic)
Vol. 47 - No. 1 - Spring 2015, pp. 55- 65

Amirkabir International Journal of Science & Research
(Modeling, Identification, Simulation & Control)
(AIJ-MISC)

Magnetic Calibration of Three-Axis Strapdown Magnetometers for Applications in Mems Attitude-Heading Reference Systems

Hamed Milanchian[1], Jafar Keighobadi[1] and Hossein Nourmohammadi[1]*
1-Department of Mechanical Engineering, University of Tabriz, Tabriz, Iran

ABSTRACT

In a strapdown magnetic compass, heading angle is estimated using the Earth's magnetic field measured by Three-Axis Magnetometers (TAM). However, due to several inevitable errors in the magnetic system, such as sensitivity errors, non-orthogonal and misalignment errors, hard iron and soft iron errors, measurement noises and local magnetic fields, there are large error between the magnetometers' outputs and actual geomagnetic field vector. This is the necessity of magnetic calibration of TAM, especially in navigation application to achieve the true heading angle. In this paper, two methodologies, including clustering swinging method and clustering velocity vector method are presented for magnetic compass calibration. Several factors for clustering process have been introduced and analyzed. The algorithms can be applied in both low-cost MEMS magnetometer and high-accuracy magnetic sensors. The proposed calibration algorithms have been evaluated using in-ground and in-flight tests. It can be concluded from the experimental results that, applying the clustering calibration algorithms bring about a considerable enhancement in the accuracy of magnetic heading angle

KEYWORDS

Magnetic Calibration, Magnetic heading angle, clustering calibration method, Swinging method, Velocity vector method.

*Corresponding Author, Email: hnourmohammadi@tabrizu.ac.ir

1. INTRODUCTION

To determine heading angle of a vehicle, three-axis MEMS magnetic compasses are widely used in low-cost attitude-heading reference systems (AHRS). In the AHRS, 3-axis orientations of a vehicle, including, attitude and heading angles are estimated. These angles are also called as Euler angles characterized by roll (φ), pitch (θ) and yaw (ψ). In order to improve the AHRS performance and accuracy, it can be integrated with the magnetic compass system. Magnetic compass comprises three-axis magnetometer which should be coupled appropriately with the inertial sensors of Inertial Measurement Unit (IMU), i.e. gyros and accelerometers [1]. Precise calibration of the TAM has a crucial effect on the attitude-heading accuracy of the AHRS systems integrated with magnetic compass. An important issue with the integrated AHRS/Magnetic systems is that the magnetic compass is greatly impressed by the environmental effects. For example, all vehicles are partially made of iron-based materials that can generate magnetic fields. Therefore, the magnetic field measured by a compass is indeed a combination of the Earth’s magnetic field, the induced magnetic field of the magnetized vehicle body and other magnetic anomalies caused by the environmental effects [2]. To estimate the heading angles of the vehicle by use of magnetic compasses, it is very necessary to filter the Earth's magnetic fields from the magnetometer measurements.

TAM Calibration should be performed due to the variation of the local magnetic effects with respect to the location, environment and operation of the onboard electronic devices. There are several methodologies for magnetic compass calibration divided into offline or online calibration and attitude independent or attitude dependent calibration [3-5]. Gebre-Egziabher et al. have estimated the calibration parameters of magnetometer, including bias and scale factor using least square estimator in the first step and algebraic estimation algorithm in the second step. In this algorithm, there is no need for using any external references and calibration has been done based on the magnetic field domain. They advanced a recursive least square estimation algorithm for magnetic calibration [6]. Wang and Gao, developed a nonlinear model for the relationship between the compass heading angle and the true heading [7]. Using neural network and estimating the model coefficients, they calibrated the magnetic compass. Kao and Tsai proposed a magnetic compass calibration algorithm based on the normalized value of GPS velocity vector [8]. Keighobadi proposed a new regression model to increase the convergence probability of the calibration process. Mamdani type fuzzy batch least-square (FBLS) algorithm was designed to estimate the calibration bias and scale factors of the magnetometers [9]. Two techniques have been proposed in [10] for fast automatic 3D-space magnetometer calibration requiring small space coverage. Theproposed techniques perform 3D-space magnetometer calibration by calibrating the three magnetometer readings in the device frame, which makes the magnetometer useful for determining heading in untethered devices, especially in pedestrian navigation There are many researches concerned with ellipsoid fitting algorithms in magnetic sensor calibration [11-14]. Given the fact that the error model of magnetic compass is an ellipsoid, Fang et al. adopted a constraint least square method to estimate the magnetic calibration parameters [11]. Kanatani et al. extended a hyper least square estimator for ellipsoid problem of TAM calibration [12]. In another work, Lou et al. realized a fast field error calibration in STM32 embedded systems Based on ellipsoid fitting algorithm [14].

Using online methods, in spite of good results, have some drawbacks to be performed. For example, an external reference signal should be available during the navigation. In the case of using GPS as the reference signal, it must be noticed that the GPS is not working properly near high buildings and natural barriers. Also, it can be interrupted by radio signals. Moreover, the online calibrations are performed with a higher level of calculations compared to offline methods. This can lead to divergence in the estimation process. Taking into account these facts, one can appreciate the necessity of periodic offline calibration algorithms. Offline calibration process brings about more convergence in the estimation algorithm. This is because of the persistently exited signals produced by the magnetometers during to continuous rotations in different orientations. In the offline methods, the external reference is required only in the calibration process and after estimating the calibration parameters, they will be used in real-time mode without any reference. However, the estimated parameters in offline methods are not global parameters.

Attitude independent algorithms usually include model based methods which are so difficult to use. In the practical applications, they frequently lead to converging and signal excitation problems. It is because of having no external reference and the only parameter reference is the magnetic field domain which is not working properly in the low-cost sensors. Attitude dependent methods are heading domain and velocity domain algorithms. The main drawback of the attitude dependent algorithms is the accuracy of attitude angles which affect the calibration, especially in airborne tests.

The main aim of the paper is to develop an efficient algorithm so as to improve the accuracy of offline and attitude dependent calibration algorithms and also wipe out the limitations and complication of online methods. Calibration parameters of each classical method do not seem to be fixed for the MEMS sensors and vary from test to test in different trajectories and maneuvers. A scheme is required to detect the dependency of calibration parameters upon test conditions. To acquire this aim, clustering calibration of TAM is proposed in the paper.

2. Strapdown Magnetic Compass System

As an aiding-navigation system, magnetic compass comprises three-axis strapdown magnetometer which detects the strength and direction of the Earth's magnetic field. Giving the horizontal plane components of the Earth's magnetic field, the magnetic heading angle can be determined. In the navigation, directions are usually expressed with respect to geographical or true north. Depending on where the magnetic compass is located on the surface of the Earth, the angle between true north and magnetic north (i.e. magnetic declination angle) can vary widely. The local magnetic declination is given on most maps, to allow the map to be oriented with a compass parallel to true north. Some magnetic compasses include means to manually compensate for the magnetic declination, so that the compass shows true directions. In the integrated AHRS/Magnetic system, TAM sensors must be mounted in aligns with the inertial sensors of the IMU. Earth's magnetic field components are measured by the TAM sensors.

$$\mathbf{M}^b = \begin{bmatrix} M_x^b & M_y^b & M_z^b \end{bmatrix}^T \tag{1}$$

in which, M_x^b, M_y^b and M_z^b are the components of magnetic field vector in the body frame (b-frame). Magnetometers' outputs can be transformed from the b-frame to navigation frame (n-frame) as follows:

$$\mathbf{M}^n = \mathbf{C}_b^n \mathbf{M}^b \tag{2}$$

where, $\mathbf{M}^n$ is the magnetic field vector in n-frame and $\mathbf{C}_b^n$ is the Direction Cosine Matrix (DCM) from the b-frame to n-frame defined with respect to the Euler angles [15].

$$\mathbf{C}_b^n = \begin{bmatrix} C\theta C\psi & -C\varphi S\psi + S\varphi S\theta C\psi & S\varphi S\psi + C\varphi S\theta C\psi \\ C\theta S\psi & C\varphi C\psi + S\varphi S\theta S\psi & -S\varphi S\psi + C\varphi S\theta S\psi \\ -S\theta & S\varphi C\theta & C\varphi C\theta \end{bmatrix} \tag{3}$$

In the horizontal plane, the magnetic vector components can be calculated as follows[16].

$$\begin{bmatrix} M_x^h \\ M_y^h \\ M_z^h \end{bmatrix} = \begin{bmatrix} \cos\theta & \sin\varphi\sin\theta & \cos\varphi\sin\theta \\ 0 & \cos\varphi & -\sin\varphi \\ -\sin\theta & \sin\varphi\cos\theta & \cos\varphi\cos\theta \end{bmatrix} \begin{bmatrix} M_x^b \\ M_y^b \\ M_z^b \end{bmatrix} \tag{4}$$

Figure (1) shows the magnetic heading angle and horizontal plane components of the magnetic field vector. Determining M_x^h and M_y^h from equation (4), the magnetic heading angle can be calculated as shown in Fig. 1.

$$\psi_m = \tan^{-1}\left(-\frac{M_y^h}{M_x^h}\right) \tag{5}$$

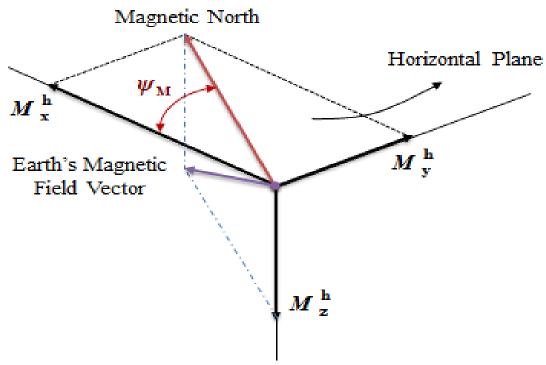

Fig. 1. Magnetic heading angle and horizontal plane components of the magnetic field vector

Due to environmental effects and external magnetic anomalies, the heading angle calculated from equations (4) and (5) is not accurate. To enhance the magnetic heading accuracy, TAM must be appropriately calibrated.

3. Calibration Algorithms

Calibration algorithms of the magnetometers can be divided into heading domain algorithms, magnetic field vector algorithms and horizontal plane's magnetic field vector algorithms. In the heading domain algorithms, the magnetic heading angle is calibrated in order to decrease the heading error of the magnetic compass. After calculating the heading angle from the magnetic field measured by TAM sensors, calibration is carried out on the computed angle. Magnetic field vector and horizontal plane's magnetic field vector algorithms calibrate each output of the TAM, directly. Giving the calibrated values of TAM's outputs, the corrected heading angle is computed. Magnetic field vector algorithms are usually model-based methods and cannot be an efficient calibration for low-cost MEMS sensors.

In the paper, two calibration methods, including clustering swinging method and clustering velocity vector method are presented. Swinging method and velocity vector method are in the category of heading domain and horizontal plane's magnetic field vector algorithms, respectively. Batched least-squares (BLS) algorithm is utilized as estimation algorithm in both calibration methods. Least-squares estimation algorithms bring about a good tracking performance because of their linear optimal features resulting from minimizing the sum of the squared prediction errors [17]. Taking into account the calculation cost offline BLS have been applied in the calibration process. Online calibrations are performed with a higher level of calculations compared to offline methods. Using any kind of online methods (model based methods, attitude dependent methods and etc.) brings about high amount of calculation due to the fact that the estimation problem is required persistently in the navigation algorithm. Using some techniques such as batch least-squares and forgetting factors, the level of calculation in least-squares algorithm is decreased. However, trying to decrease the calculations often leads to divergence in the estimation process. For instance small batches in a least square estimator may result in a regressor matrix that doesn't satisfy a high order of persistent excitation.

A. Swinging Method

In the swinging method, calibration is carried out based on the perturbation of equation (5), the basic magnetic heading equation. The following equation is defined as the heading error equation.

$$\delta\psi = A + B\sin(\hat{\psi}_m) + C\cos(\hat{\psi}_m) + D\sin(2\hat{\psi}_m) + E\cos(2\hat{\psi}_m) \qquad (6)$$

Equation (6) is a reduced-order Fourier series in which the coefficients A, B, C, D and E are functions of the hard and soft iron errors [18]. The procedure for estimation of the Fourier coefficients is so-called "swinging". This involves leveling and rotating the vehicle containing the magnetometer through a series of N known headings. The heading error $\delta\psi$ is computed for each known heading as follows:

$$\delta\psi = \psi_{ref} - \hat{\psi}_m \qquad (7)$$

where ψ_{ref} is the reference value of the heading angle. Eventually, the following regression model can be constituted for all of the N measurements.

$$\begin{bmatrix} \delta\psi_1 \\ \delta\psi_2 \\ \vdots \\ \delta\psi_N \end{bmatrix} = \begin{bmatrix} 1 & \sin\hat{\psi}_1 & \cos\hat{\psi}_1 & \sin 2\hat{\psi}_1 & \cos 2\hat{\psi}_1 \\ 1 & \sin\hat{\psi}_2 & \cos\hat{\psi}_2 & \sin 2\hat{\psi}_2 & \cos 2\hat{\psi}_2 \\ \vdots & \vdots & \vdots & \vdots & \vdots \\ 1 & \sin\hat{\psi}_N & \cos\hat{\psi}_N & \sin 2\hat{\psi}_N & \cos 2\hat{\psi}_N \end{bmatrix} \begin{bmatrix} A \\ B \\ C \\ D \\ E \end{bmatrix} \qquad (8)$$

Using BLS algorithm [19], the coefficients A through E can be estimated from equation (8). Instead of leveling and rotating, the vehicle can be traveled through a specified trajectory called calibration track as shown in Fig. 2.

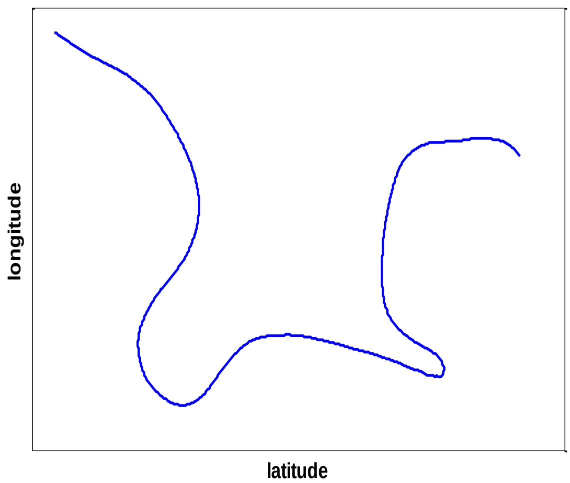

Fig. 2. Calibration track with known heading angle

The reference heading angle would be available throughout the calibration track by use of an aiding navigation system such as GPS or accurate INS. Using the reference heading angle, the calibration parameters in equation (6) are determined. Finally, the corrected value of magnetic heading angle will be estimated through the following equation.

$$\psi_c = A + B\sin(\hat{\psi}_m) + C\cos(\hat{\psi}_m) + D\sin(2\hat{\psi}_m) + E\cos(2\hat{\psi}_m) + \hat{\psi}_m \qquad (9)$$

B. Velocity Vector Method

In the velocity vector method, calibration is carried out based on the horizontal plane magnetic field vector. A reference value for velocity vector is required in this algorithm. Giving the velocity component in the east and north direction, the vehicle heading can be determined by equation (10).

$$\psi_v = \tan^{-1}\left(\frac{V^{east}}{V^{north}}\right) \quad (10)$$

And the normalized velocity vector can be found as follows:

$$(u_E, u_N) = (\sin\psi_v, \cos\psi_v) \quad (11)$$

In the case of using GPS velocity to get the reference heading angle, some considerations must be adopted. In the GPS receivers, the velocity vector is measured based on the Doppler frequency or pseudo-range rate [20]. GPS track angle would be corrupted by the measurement noises at low speed. Therefore, the vehicle should be moved at reasonable speed to acquire good calibration. In addition, signal blockage in urban environments would affect the heading accuracy.

Defining bias and scale factor, the horizontal components of the magnetic field vector can be modeled by equation (12).

$$\begin{aligned} \hat{M}_x^h &= G_x^h (M_x^h + C_x^h) \\ \hat{M}_y^h &= G_y^h (M_y^h + C_y^h) \end{aligned} \quad (12)$$

where, $\hat{M}_y^h$ and $\hat{M}_y^h$ are the horizontal components of TAM's outputs. M_x^h and M_y^h are true values of the magnetic field. C^h and G^h are bias and scale factor, respectively. Equation (12) can be rewritten as follows:

$$\begin{aligned} m_x^h &= \hat{M}_x^h k_x^h - B_x^h \\ m_y^h &= \hat{M}_y^h k_y^h - B_y^h \end{aligned} \quad (13)$$

In equation (13) unit vector components of the horizontal magnetic field are specified by m_x^h and m_y^h. As shown in Fig. 3, m_x^h and m_y^h are expressed with respect to u_N and u_E by equation (14).

$$\begin{bmatrix} m_y^h \\ m_x^h \end{bmatrix} = \begin{bmatrix} \cos(-\delta) & \sin(-\delta) \\ -\sin(-\delta) & \cos(-\delta) \end{bmatrix} \begin{bmatrix} u_E \\ u_N \end{bmatrix} \quad (14)$$

where, δ is the declination angle.

Assuming small declination angle, the following regression model can be derived for the velocity vector method based on equations (12) – (14).

$$\begin{bmatrix} u_E \\ u_N \end{bmatrix} = \begin{bmatrix} 0 & \hat{M}_y^h & 0 & -1 & u_N \\ \hat{M}_x^h & 0 & -1 & 0 & -u_E \end{bmatrix} \begin{bmatrix} k_x^h \\ k_y^h \\ B_x^h \\ B_y^h \\ \delta \end{bmatrix} \quad (15)$$

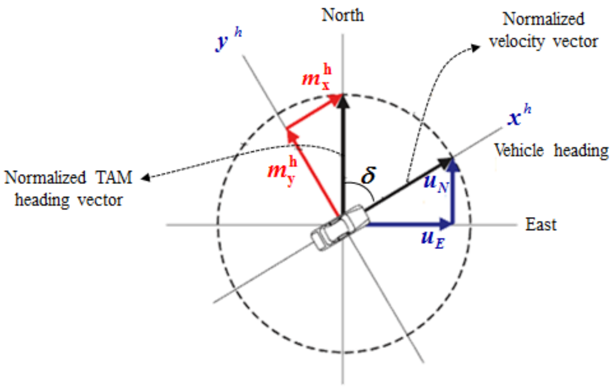

Fig. 3. TAM heading vector and normalized velocity vector

Using least square algorithm the calibration parameters can be found. Horizontal components of the magnetic field unit vector can be found based on equation (13). Giving m_x^h and m_y^h, magnetic heading angle can be calculated by equation (1). Eventually, the calibrated heading angle in this method would be determined by adding the declination angle to the magnetic heading angle as follows:

$$\psi_c = \psi_m + \delta \quad (16)$$

C. Clustering Calibration Methods

In spite of the good accuracy of online magnetic calibration, there are some drawbacks that restrict the practical application of online TAM calibration in the magnetic compass. High amount of calculation and necessity of reference signal availability are the main drawbacks of online calibration. On the other hand, using offline methods did not require much calculation. However, it has lower accuracy. Bearing in mind these facts, one can appreciate the importance of advancing an accurate calibration algorithm, especially for navigation purposes.

Calibration parameters of each classical method do not seem to be fixed for the MEMS sensor and vary from test to test in different trajectories and maneuvers. A scheme was required to detect the dependency of calibration parameters upon test conditions. To acquire this aim, clustering calibration of TAM is proposed in the paper.

Every test has its own conditions, such as acceleration, angular rates and domain of headings. In the clustering calibration method, the test data is divided into several classes, and each class is named a cluster. Test classification is done based on the vehicle maneuvering. Calibration parameters of swinging method and vector velocity method are determined for each cluster. The clustered calibration parameters could be used in any other test with pre-obtained conditions. Updating classic swinging method and classic vector velocity with clustering swinging method and clustering vector velocity method would enhance the performance and accuracy of offline calibration of the magnetic compass. Schematic view of the proposed clustering calibration method is depicted in Fig. 4. Maneuver intensity of the vehicle's motion throughout the calibration track can be specified based on different factors, including norm of the rate vector $(\boldsymbol{\omega}^b)$, norm of the acceleration vector $(\boldsymbol{a}^b)$, norm of the magnetic field vector $(\boldsymbol{M}^b)$, heading angle (ψ), y-component of the acceleration vector (a_y^b) and the angular velocity about the z-axis (ω_z^b). Rate vector and acceleration vector are dynamical properties of the vehicle's motion. So, they can be a good factor for data clustering. Magnetic field vector is chosen due to the fact that its norm is ideally constant in a specific area. However, because of magnetic anomalies and other effects, it is not so. Hence, Clustered parameters for different magnitudes of $\boldsymbol{M}^b$ is suggested. Heading angle is chosen, because calibration parameters may vary according to heading angles. a_y^b and ω_z^b are the main factors of changing the heading angles. So, they can be efficient factors in the clustering process.

The procedure for clustering calibration method is in a way that, one of the mentioned factors (e.g. $\boldsymbol{\omega}^b$) is analyzed in a specified calibration test trajectory and clusters are created (3 to 5 clusters are suggested). All TAM data will be classified in these clusters. Calibration process (swinging method or vector velocity method) will be carried out individually in each cluster. Finally, the calibration parameters corresponding to each cluster will be estimated. The efficiency of the clustering factors in the calibration accuracy will be surveyed in the next section.

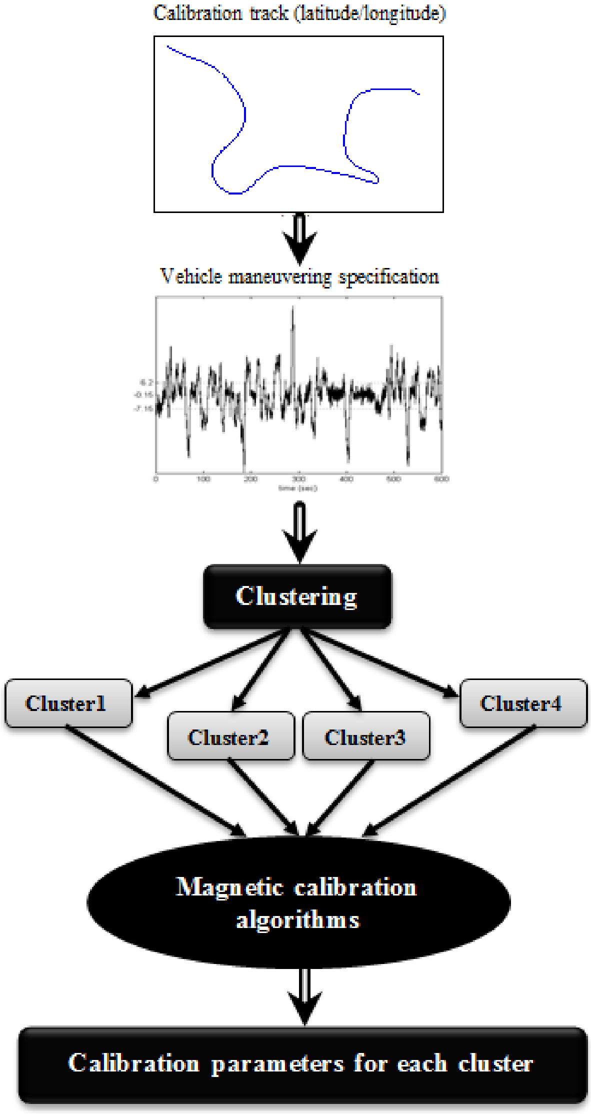

Fig. 4. Schematic view of the proposed clustering calibration method

4. Experimental Results And Discussion

In order to assess the performance of the presented TAM calibration algorithm, several experimental tests have been exerted on both ground and airborne vehicles. The algorithm has been evaluated in two in-ground in-flight tests.

A. In-Ground Test

The in-ground test has been executed in the campus of the University of Tabriz. Experimental data were logged through ANALOG DEVICE ADIS16407 IMU sensors comprised of accelerometers, gyros and magnetometers. In addition, a GARMIN GPS receiver and VITANS INS have been used during the test in order to provide the reference data. In the experiment, it must be noticed that, the magnetic sensors should not be so close to ferrous metals. Taking into account this fact, the IMU which contains the magnetometers was mounted on an aluminum profile far away the vehicle's body as shown in Fig. 5.

Vehicle's motion throughout the test trajectory is divided into two parts: calibration track and evaluation track. In the course of calibration track, the reference data is available. Calibration process is executed for this part of the test trajectory. After finishing the calibration track, the results are evaluated over the evaluation track. This track is just for assessing the accuracy of the proposed offline calibration algorithm. The calibration track lasts 200 seconds and evaluation duration is 300 seconds. To analyze to the calibration accuracy, heading error is defined as follows:

$$\delta\psi = \psi_{ref} - \psi_c \tag{17}$$

where, ψ_c is the calibrated magnetic heading angle and ψ_{ref} is the reference value of the heading angle. The heading error will be calculated in both calibration and evaluating track. In the perfect mode, the heading error converges to zero. So the mean and RMS values of heading error signal should be zero for a good calibration process. However, because of system noises and magnetic disturbances, this is not fully reachable.

The calibration and evaluation tracks in the in-ground test are depicted in Fig. 6. The results are shown in Tab. 1 and Tab. 2. The mean and RMS values of heading error would be calculated in all tracks. However, in order to assess the proposed algorithm, the evaluation track is more important compared to calibration track.

Table (1) shows the performance of the swinging calibration method. Without applying calibration process, 6.26 deg of mean value and 19.96 deg of RMS value are obtained for heading error in the calibration track. Using classic swinging method, these values are reduced to zero mean and 4.84 deg RMS. In the evaluation track, the heading error reaches the mean value of -1.4 deg and RMS value of 7.14 deg. Therefore, the calibration parameters estimated in the calibration track result in a good performance in the evaluation track. Among the clustering factors, ω_z^b clustering has the best accuracy. ω_z^b Clustering method not only reduces the RMS value to 4.34 deg in the calibration track, but also has a mean value of -1.33 deg and RMS value of 6.36 deg in the evaluation track.

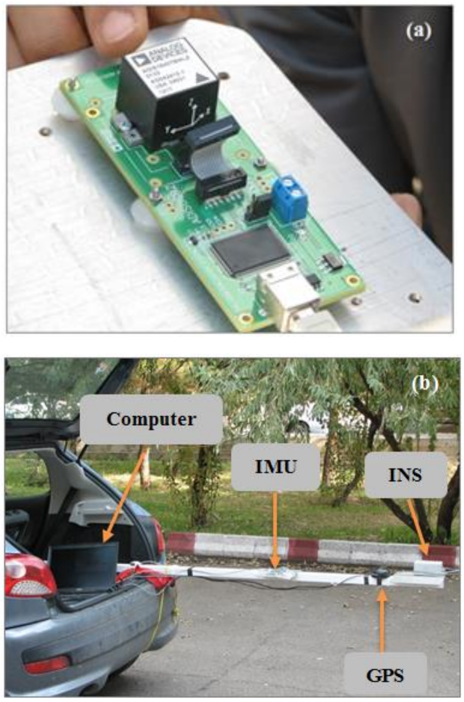

Fig. 5. (a) IMU-ADIS16407, (b) Experiment devices placed on the vehicle

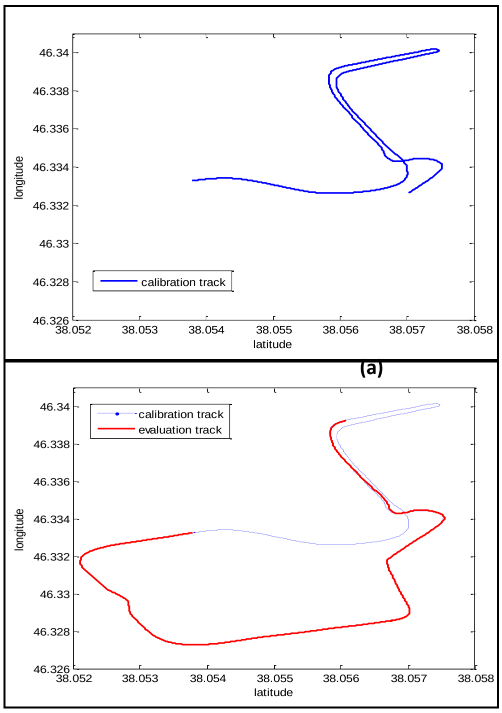

Fig. 6. In-ground test, (a) Calibration track, (b) Evaluation track

TABLE 1. THE RESULTS OF THE SWINGING CALIBRATION ALGORITHM IN THE IN-GROUND TEST

		Calibration		***Evaluation***	
		$\delta\psi$		$\delta\psi$	
		Mean (deg)	***RMS (deg)***	***Mean (deg)***	***RMS (deg)***
Without calibration		*6.26*	*19.96*	*14.84*	*21.87*
Classic calibration		*0*	*4.84*	*-1.40*	*7.14*
Clustering based on:	$\hat{\psi}_m$	*0*	*4.40*	*-2.94*	*8.53*
	$\boldsymbol{\omega}^b$	*0*	*4.75*	*-1.56*	*7.32*
	$\boldsymbol{a}^b$	*0*	*4.83*	*-1.41*	*7.15*
	$\boldsymbol{M}^b$	*0*	*4.48*	*-2.00*	*7.76*
	a_y^b	*0*	*4.60*	*-1.57*	*7.04*
	ω_z^b	*0*	*4.34*	*-1.33*	*6.36*

Similar results have been obtained for the velocity vector method as shown in Tab. 2. The classic velocity vector algorithm has a mean value of 0.04 deg and RMS value of 5.03 deg in the calibration track. In the evaluation track, these values are -0.81 deg and 6.89 deg, respectively. Like swinging method, ω_z^b clustering method has the best results in both calibration and evaluation tracks.

TABLE 2. . THE RESULTS OF THE VELOCITY VECTOR CALIBRATION ALGORITHM IN THE IN-GROUND TEST

		Calibration		***Evaluation***	
		$\delta\psi$		$\delta\psi$	
		Mean (deg)	***RMS (deg)***	***Mean (deg)***	***RMS (deg)***
Without calibration		*6.26*	*19.96*	*14.84*	*21.87*
Classic calibration		*0.04*	*5.03*	*-0.81*	*6.89*
Clustering based on:	$\hat{\psi}_m$	*0.10*	*4.40*	*-1.49*	*8.04*
	$\boldsymbol{\omega}^b$	*0.05*	*4.99*	*-0.99*	*7.04*
	$\boldsymbol{a}^b$	*0.04*	*5.02*	*-0.81*	*6.90*
	$\boldsymbol{M}^b$	*0.03*	*4.53*	*-1.34*	*7.18*
	a_y^b	*0.05*	*4.88*	*-1.06*	*6.69*
	ω_z^b	*0.06*	*4.73*	*-0.81*	*6.14*

Due to heading domain calibration in the swinging algorithms, zero mean heading errors are achieved in the calibration track. But, the mean values are not so close to zero in the evaluation track. In velocity vector method, the calibration process is executed on the horizontal components of the magnetic field vector. So, the mean values of heading error in calibration track are not exactly zero like swinging method. However, velocity vector method has a better performance compared to swinging method as velocity vector method nearly repeats those mean values in evaluation track. It must be noticed that, the calibration track plays a key role in the offline calibration. The vehicle's maneuver in the calibration track must be rich enough to results in a good accuracy of the calibration parameters.

B. In-Flight Test

In order to make a certain decision about the performance of the proposed calibration method, the algorithms are also evaluated in the airborne test. The calibration and evaluation tracks in the in-flight test are depicted in Fig. 7. The MEMS magnetometers that have been used in the airborne test are not the same as the sensors used in the car test.

After calibrating the magnetic system, the estimated calibration parameters have been applied to both calibration and evaluation tracks and the results are shown in Tab. 3 and Tab. 4. The main difference between car and airborne tests is the maneuver's characteristics. The variation of tilt angles of the vehicle will be higher in the car test. Therefore, the accuracy of roll and pitch angles for transforming the magnetometers' outputs from the body frame to the horizontal plane (see equation (4)) is more important to get a better calibration process.

Without applying any calibration algorithms, the heading errors in the airborne test are lower compared to those of the car test. This is due to different magnetic sensors used in the airborne test. Both standard methods of swinging and velocity vector algorithms have heading errors so close to non-calibrated heading error signal. Classic swinging and velocity vector calibrations results in 11.56 deg RMS value and 10.88 deg RMS value in the evaluation track which are so close to 11.57 degree.

Among the clustering methods, clustering based on the ω_z^b leads to the best performance. Clustering swinging method based on ω_z^b has zero mean and 6.16 deg RMS

TABLE 3. THE RESULTS OF THE SWINGING CALIBRATION ALGORITHM IN THE IN-FLIGHT TEST

		Calibration		*Evaluation*	
		$\delta\psi$		$\delta\psi$	
		Mean (deg)	*RMS (deg)*	*Mean (deg)*	*RMS (deg)*
Without calibration		***-2.60***	***14.04***	***-1.97***	***11.57***
Classic calibration		***0***	***10.32***	***3.70***	***11.56***
Clustering based on:	$\hat{\psi}_m$	***0***	***9.43***	***7.81***	***15.98***
	$\boldsymbol{\omega}^b$	***0***	***10.01***	***3.08***	***10.47***
	$\boldsymbol{a}^b$	***0***	***9.97***	***2.84***	***10.65***
	$\boldsymbol{M}^b$	***0***	***8.04***	***5.23***	***13.93***
	a_y^b	***0***	***9.93***	***3.46***	***11.65***
	ω_z^b	***0***	***6.16***	***1.11***	***7.86***

TABLE 4. THE RESULTS OF THE VELOCITY VECTOR CALIBRATION ALGORITHM IN THE IN-FLIGHT TEST

		Calibration		**Evaluation**	
		$\delta\psi$		$\delta\psi$	
		Mean (deg)	*RMS (deg)*	*Mean (deg)*	*RMS (deg)*
Without calibration		-2.60	14.04	-1.97	11.57
Classic calibration		***-0.80***	***13.31***	***-1.95***	***10.88***
Clustering based on:	$\hat{\psi}_m$	*0.06*	*9.34*	*7.16*	*15.78*
	$\boldsymbol{\omega}^b$	*-0.78*	*12.91*	*-0.67*	*11.51*
	$\boldsymbol{a}^b$	*-0.74*	*12.93*	*-2.22*	*10.71*
	$\boldsymbol{M}^b$	*0.32*	*9.28*	*-0.85*	*12.73*
	a_y^b	*-0.75*	*12.97*	*-1.97*	*10.91*
	ω_z^b	*-0.12*	*7.94*	*-1.49*	*7.71*

Value in the calibration track and 1.11 deg mean value and 7.86 deg RMS value in evaluation track. Applying clustering velocity vector, mean values reach to -0.12 deg and -1.49 deg in the calibration and evaluation tracks and the RMS values are 7.94 deg and 7.71 deg.

Considering experimental results of both in-ground and in-flight tests, it can be concluded that like $\omega^b{}_z$ clustering method has the best accuracy in the different maneuvers and different magnetic sensors.

The effects of some nonlinear phenomena such as hysteresis and saturation have been entered in the form of bias and scale factor. However, due to inaccessibility of analog and raw data of magnetometers, they cannot be detected directly. Therefore, the impact of such phenomena on the data obtained from ADC converter along with the other noises and anomalies has been identified and compensated as calibration parameters.

5. CONCLUSION

In the low-cost AHRS, it is very difficult to estimate the heading angle with an acceptable precision. This is because of using low-precision MEMS inertial sensors (i.e. gyros and accelerometers), modeling and parameter uncertainties as well as the filter algorithm complexity. To overcome this drawback, integrated AHRS/Magnetic system is proposed. Using magnetic compass as an aiding-navigation system, the accuracy of heading angle estimated in the low-cost AHRS will be enhanced. On the other hand, the magnetic compass is impressed by magnetic anomalies and induced magnetic fields as external disturbances. Therefore, magnetic compass calibration is very essential to achieve a good accuracy in the heading angle. In this paper, a novel method for offline calibration of the MEMS magnetic compass system was proposed. Based on swinging method and velocity vector method, two different methodologies have been developed in the paper. In order to enhance the accuracy of offline magnetic calibration, the classic swinging and velocity vector algorithms were extended to clustering ones. Several clustering factors, including rate vector, acceleration vector, magnetic field vector, heading angle, y-components of the acceleration and angular velocity about the z-axis have been presented. The efficiency of each factor on the calibration accuracy has been surveyed. According to experimental results, it can be concluded that the clustering based on ω_z^b leads to the best performance in both swinging and velocity vector methods.

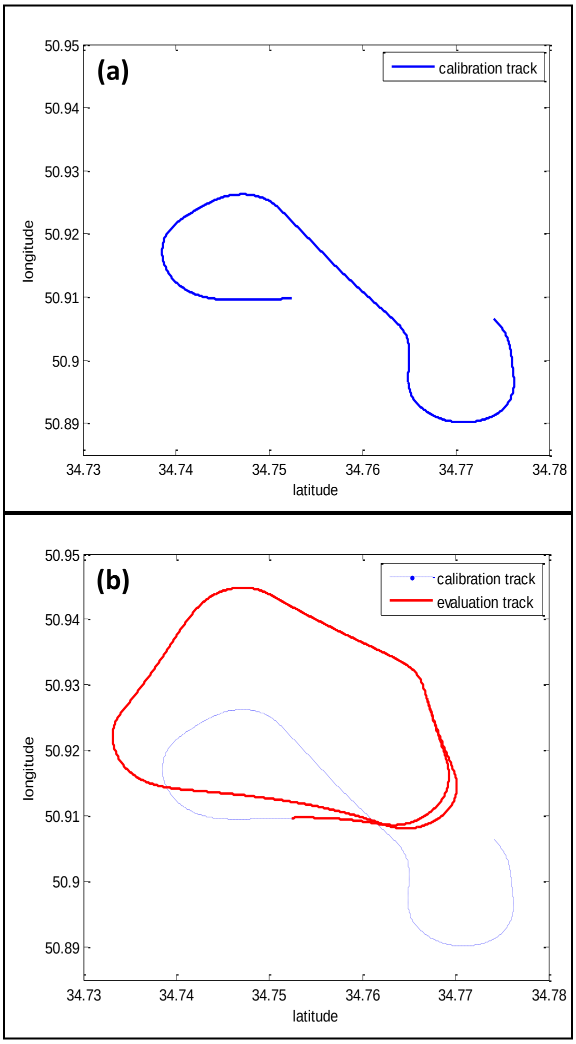

Fig. 7. In-flight test, (a) Calibration track, (b) Evaluation track

REFERENCES

[1] Alandry, B., et al., "A fully integrated inertial measurement unit: application to attitude and heading determination," Sensors Journal, IEEE, vol. 11, no. 11, pp. 2852-2860, 2011.

[2] Storms, W., J. Shockley, and J. Raquet, "Magnetic field navigation in an indoor environment," Ubiquitous Positioning Indoor Navigation and Location Based Service (UPINLBS), 2010: IEEE, 2010.

[3] Crassidis, J.L., K.-L. Lai, and R.R. Harman, "Real-time attitude-independent three-axis magnetometer calibration," Journal of Guidance, Control, and Dynamics, vol. 28, no.1, pp. 115-120, 2005.

[4] Han, S. and J. Wang, "A novel method to integrate IMU and magnetometers in attitude and heading reference systems," Journal of Navigation, vol. 64, no. 04, pp. 727-738, 2011.

[5] Wahdan, A., et al., "Magnetometer calibration for portable navigation devices in vehicles using a fast and autonomous technique," Intelligent Transportation Systems, IEEE Transactions on, vol. 15, no. 5, pp. 2347-2352, 2014.

[6] Gebre-Egziabher, D., et al., "Calibration of strapdown magnetometers in magnetic field domain," Journal of Aerospace Engineering, vol. 19, no. 2, pp. 87-102, 2006.

[7] Wang, J.-H. and Y. Gao, "A new magnetic compass calibration algorithm using neural networks," Measurement Science and Technology, vol. 17, no. 1, pp. 153, 2006.

[8] Kao, W.-W. And C.-L. Tsai, "Adaptive and learning calibration of magnetic compass," Measurement Science and Technology, vol. 17, no. 11, pp. 3073, 2006.

[9] Keighobadi, J., "Fuzzy calibration of a magnetic compass for vehicular applications," Mechanical Systems and Signal Processing, vol. 25, no. 6, pp. 1973-1987, 2011.

[10] Wahdan, A., J. Georgy, and A. Noureldin, "Three-Dimensional Magnetometer Calibration with Small Space Coverage for Pedestrians," Sensors Journal, IEEE, vol. 15, no.1, pp. 598-609, 2015.

[11] Li, X. and Z. Li, "A new calibration method for tri-axial field sensors in strap-down navigation systems," Measurement Science and technology, vol. 23, no. 10, pp. 105105, 2012.

[12] Kanatani, K. and P. Rangarajan, "Hyper least squares fitting of circles and ellipses," Computational Statistics & Data Analysis, vol. 55, no. 6, pp. 2197-2208, 2011.

[13] Feng, W., et al., "A calibration method of three-axis magnetic sensor based on ellipsoid fitting," J. Inf. Comput. Sci, vol. 10, pp. 1551-1558, 2013.

[14] Lou, X., L. Zhou, and Y. Jia, "Realization of Ellipsoid Fitting Calibration for Three-Axis Magnetic Sensor Based on STM32 Embedded System, in Human Centered Computing," Springer, pp. 717-726, 2015.

[15] Titterton, D. and J.L. Weston, "Strapdown inertial navigation technology," vol. 17: IET, 2004.

[16] Li, W. and J. Wang, "Effective adaptive Kalman filter for MEMS-IMU/magnetometers integrated attitude and heading reference systems," Journal of Navigation, vol. 66, no. 01, pp. 99-113, 2013.

[17] Li, W. and J. Wang, "Effective adaptive Kalman filter for MEMS-IMU/magnetometers integrated attitude and heading reference systems," Journal of Navigation, vol. 66, no. 01, pp. 99-113, 2013.

[18] Guo, P., et al. "The soft iron and hard iron calibration method using extended kalman filter for attitude and heading reference system," Position, Location and Navigation Symposium, IEEE/ION. 2008: IEEE, 2008.

[19] Simon, D., Optimal state estimation: Kalman, H infinity, and nonlinear approaches, John Wiley & Sons, 2006.

[20] Bevly, D.M., et al., "The use of GPS based velocity measurements for improved vehicle state estimation," American Control Conference,. Proceedings of the 2000. 2000: IEEE, 2000.